

Absence of electron-phonon-mediated superconductivity in hydrogen-intercalated nickelates

Simone Di Cataldo ^{1,†} Paul Worm ¹ Liang Si ^{2,1} and Karsten Held ¹

¹*Institut für Festkörperphysik, Technische Universität Wien, 1040 Wien, Austria*

²*School of Physics, Northwest University, Xi'an 710127, China*

(Dated: April 10, 2023)

A recent experiment [X. Ding *et al.*, Nature 615, 50 (2023)] indicates that superconductivity in nickelates is restricted to a narrow window of hydrogen concentration: $0.22 < x < 0.28$ in $\text{Nd}_{0.8}\text{Sr}_{0.2}\text{NiO}_2\text{H}_x$. This reported necessity of hydrogen suggests that it plays a crucial role for superconductivity, as it does in the vast field of hydride superconductors. Using density-functional theory and its extensions, we explore the effect of topotactic hydrogen on the electronic structure and phonon-mediated superconductivity in nickelate superconductors. Our calculations show that the electron-phonon coupling in hydrogen-intercalated nickelates is not strong enough to drive the electron pairing, and thus cannot explain the reported superconductivity.

Our understanding of the pairing mechanism and gap function in the recently synthesized nickelate superconductors [1–6] is still in its infancy, and it goes without saying that it is controversially debated. Scanning tunneling microscopy (STM) shows both a “U” and a “V” shape gap [7], depending on the precise position of the tip on the surface and indicative of a *d*- and *s*-wave gap, respectively. Fits to the London penetration depth either point to a nodeless [8] or a nodal [9] gap.

Theories range from *d*-wave superconductivity originating from spin-fluctuations in the Ni $d_{x^2-y^2}$ orbital [10–13] to two-orbital physics with *d*- and s_{\pm} -wave superconductivity [14]. Also superconductivity based on a Kondo coupling between Ni-spin and Nd-bands [15], the importance of the inter-orbital Coulomb interaction [16], and a possible connection to charge ordering [17] have been suggested, among others.

Early calculations [18, 19] indicated that topotactic hydrogen might be intercalated when reducing $\text{Nd}_{0.8}\text{Sr}_{0.2}\text{NiO}_3$ to $\text{Nd}_{0.8}\text{Sr}_{0.2}\text{NiO}_2$ with the reagent CaH_2 [20]. The presence of hydrogen in nickelates has by now been established using nuclear magnetic resonance (NMR) [21] in film samples and using neutron scattering [22] in bulk LaNiO_2 , where H appears to cluster at the grain boundaries.

The work by Ding *et al.* [23] now prompts for a complete overhaul of our picture of superconductivity in nickelates. Systematically increasing the exposure time to CaH_2 and using ion mass spectroscopy, Ding *et al.* link the occurrence of superconductivity to a narrow range of hydrogen concentration $0.22 < x < 0.28$. Most notably, superconductivity seems absent for low hydrogen concentrations, implying that its presence is necessary for superconductivity. Arguably the most obvious –but hitherto for nickelates unexplored– route for hydrogen to cause superconductivity is via the conventional, electron-phonon (*ep*) mechanism. Due to its light mass, hydrogen can lead to high-temperature superconductivity, with critical temperatures (T_c) up to almost room temperature in hy-

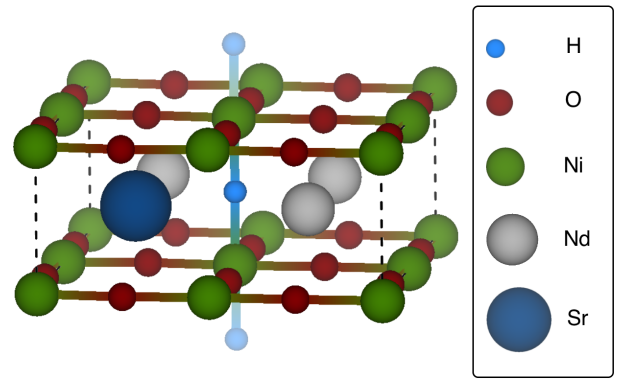


FIG. 1. $2 \times 2 \times 1$ supercell for $\text{Nd}_{0.75}\text{Sr}_{0.25}\text{NiO}_2\text{H}_{0.25}$ with the experimentally optimal hydrogen concentration [23]. The hydrogen chain is indicated by two additional H atoms outside the supercell; atoms at the surface, edge, and corner count by a factor of 1/2, 1/4 and 1/8 respectively.

drides under pressure [24–28]. Furthermore, the *s*-wave-gap reported in Ref. [14] might be naturally explained from such an *ep* mechanism. In this context, a hydrogen *ep* mechanism for at least some of the superconductivity in nickelates appears to be a very reasonable and appealing working hypothesis. Let us also note that the *ep* mechanism for nickelate superconductors without hydrogen has been explored previously, but does not result in sizable T_c 's within density-functional theory (DFT) [29].

In this letter, we thus explore the hydrogen *ep* scenario for $\text{Nd}_{0.75}\text{Sr}_{0.25}\text{NiO}_2\text{H}_{0.25}$ which is exactly at the optimum of Ding *et al.* [23]. Since it is energetically favorable for hydrogen to form chains [30, 31], the simplest structure compatible with the experimental observation is one hydrogen (chain) in a $2 \times 2 \times 1$ supercell, see Fig. 1. This supercell can also accommodate 25% Sr doping, close to the experimentally investigated 20% and still in the range of superconducting dome [1, 3, 32]. We investigated the electronic and vibrational properties by means of DFT

[33] and density-functional perturbation theory (DFPT) [34], respectively. We find however that the electron-phonon (ep) coupling is minimal, and cannot explain the reported T_c 's. Furthermore, engineering optimal conditions for ep superconductivity by changing the rare earth to La and performing a comprehensive study of different hydrogen concentrations does not yield any finite transition temperature either. We thus conclude that the measured T_c eludes an explanation in terms of a simple boost in the ep coupling driven by hydrogen.

Methods: DFT. All DFT calculations were performed using Quantum ESPRESSO version 7.1, employing optimized norm-conserving Vanderbilt pseudopotentials [35, 36]. The pseudopotential of neodymium uses the frozen-core approximation for the f states. We used a 90 Ry cutoff on the plane-waves expansion, and $8 \times 8 \times 8$ grid with a 0.040 Ry smearing for Brillouin zone integration. The crystal structures were constructed using VESTA [37] and subsequently relaxed until forces (stresses) were lower than 10^{-5} Ry/Bohr (0.5 kBar). Due to the larger size of Sr compared to Nd a local distortion of the Ni-O-Ni bond angle is induced, which deviates from 180 to 172° around Sr to accommodate the atom; see Supplementary Material [38] Fig. S1.

Phonon calculations were performed on a Γ -centered $2 \times 2 \times 2$ grid, within the harmonic approximation. Anharmonic corrections were introduced for specific modes using the frozen-phonon approach presented in [39] (further details are available in the Supplemental Material [38]). The integral of the electron-phonon matrix elements was performed on a $16 \times 16 \times 16$ and $24 \times 24 \times 24$ grid. A Gaussian smearing of 100 meV was found to give a converged result. The rigid-band approximation for the integration of the ep matrix elements was performed using our modified version of Quantum ESPRESSO [40].

Methods: McMillan formula. In a conventional ep superconductor the superconducting T_c can be estimated by the McMillan formula [41, 42], which works particularly well in the weak-coupling regime:

$$T_c = \frac{\omega_{log}}{1.2} \exp \left[\frac{1.04(1 + \lambda)}{\lambda - \mu^*(1 + 0.62\lambda)} \right] \quad (1)$$

where λ and ω_{log} describe the average strength of the ep coupling and phonon energies, respectively. It is apparent from Eq. 1 that high T_c 's require a combination of both (i) strong ep coupling (large λ) and (ii) high phonon energy (large ω_{log}). Generally speaking, hydrogen can boost both of these quantities as phonons involving it are typically high-energy and unscreened; and hydrogen-rich conventional superconductors have indeed reached extremely high T_c 's [24–28].

Fermi surface nesting for $\text{Nd}_{0.75}\text{Sr}_{0.25}\text{NiO}_2\text{H}_{0.25}$ was computed using the EPW code [43, 44], with a Wannier interpolation over a $32 \times 32 \times 32$ grid (for further details on the wannierization we refer the reader to the Supplemental Material [38]). In $\text{Nd}_{0.75}\text{Sr}_{0.25}\text{NiO}_2\text{H}_{0.25}$ EPW

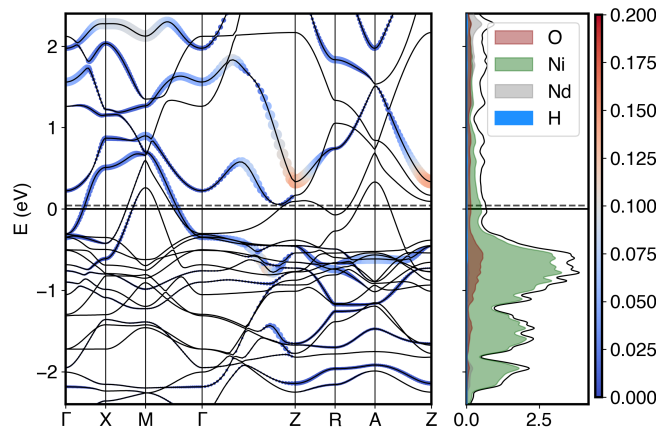


FIG. 2. left: Electronic band structure of $\text{Nd}_{0.75}\text{Sr}_{0.25}\text{NiO}_2\text{H}_{0.25}$, decorated with the orbital projection onto the H-1s state. Right: Total and atom-projected density of states. The size and color scale of the colored bands (left) indicates the H fraction of states, from 0 to 0.20. The Fermi energy for 25% and 20% Sr doping is shown as a solid black and dashed gray line, respectively. The DOS (right) is in units of states/eV/f.u. The atom projection onto Nd(+Sr), Ni, O, and H is shown as gray, green, red, and blue-filled curves, respectively.

was also used to provide an additional convergence test of ep properties by interpolating the ep matrix elements over a $12 \times 12 \times 12$ and $24 \times 24 \times 24$ grid for phonons and electrons, respectively, still yielding a T_c of 0 K.

Electronic structure. In Fig. 2 we show the electronic band structure (left) decorated with the hydrogen 1s character, and the orbital resolved density of states (right) of $\text{Nd}_{0.75}\text{Sr}_{0.25}\text{NiO}_2\text{H}_{0.25}$ (a comparison with the band structure of the parent compound $\text{Nd}_{0.75}\text{Sr}_{0.25}\text{NiO}_2$ is shown in the Supplemental Material [38] Figure S2; it has also been calculated before e.g. in [10, 15, 29, 45]). The presence of topotactic hydrogen opens a wide gap around the Z point, slightly above the Fermi energy, and another one in the band going from Γ to Z. These bands can be identified easily since they present a significant hydrogen character. Due to its low concentration relative to the other elements, hydrogen contributes to only about 2% of the DOS at the Fermi level. A band with significantly higher hydrogen character is present along the Γ -Z direction, at about 0.5 eV above the Fermi energy, which is, however, too high to contribute significantly to superconductivity.

The Fermi surface consists of three sheets (shown in Supplemental Material [38] Fig. S3): a long, tubular sheet forming an electron pocket around Γ , and similar hole pockets around M , elongated along the k_z direction. None of these sheets presents significant hydrogen character, which is rather evenly spread over all wavevectors.

Electron-phonon superconductivity. To establish whether the presence of hydrogen leads to a significant superconducting T_c via the conventional ep mecha-

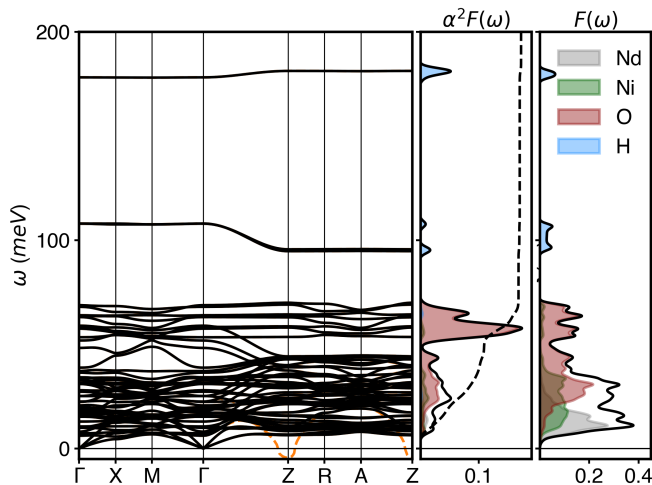


FIG. 3. Phonon dispersions (left), atom-projected Eliashberg function ($\alpha^2F(\omega)$; middle), and phonon density of states ($F(\omega)$; right). In the harmonic approximation, there is an instability at the Z point (orange dashed orange lines), which is removed when including the anharmonic correction at this point (black solid lines). The total phonon DOS and Eliashberg function are shown as black solid lines, while projections onto Nd(+Sr), Ni, O, and H are shown as gray-, green-, red-, and blue-filled curves.

nism, we computed the superconducting properties using DFPT as implemented in Quantum ESPRESSO [46–48]. In Fig. 3 we report the phonon dispersions along with the atom-projected phonon density of states and the Eliashberg function.

The phonon dispersion is characterized by two rather flat branches at about 110 and 180 meV, which correspond to the twofold-degenerate in-plane (Nd-H) and out-of-plane (Ni-H) hydrogen vibrations. In addition, a single mode involving in-plane bending of the Ni-O bond presents a small imaginary frequency at the Z point. Inclusion of anharmonic effects via a frozen-phonon approach as in [39] is enough to remove this instability, as the anharmonic mode goes from $6i$ to 9 meV [49]. Using the same approach, we computed the anharmonic vibrational frequency for the Ni-H and Nd-H modes at the Γ point. In the Ni-H mode, we observe a hardening of the mode from 178 to 191 meV, while for the Nd-H mode, we found the anharmonic frequency at 113 meV is only 5 meV higher than the harmonic result. To check the possible influence of anharmonicity on the ep coupling, we diagonalized the dynamical matrix and computed the coupling both with and without it, but found no significant change in our results.

The phonon modes involving Ni-H and Nd-H exhibit only an extremely small ep coupling and thus essentially do not contribute to superconductivity. Indeed, the integrated ep coupling and average phonon frequency are $\lambda = 0.16$ and $\omega_{log} = 43.4$ meV, respectively. This means that the superconducting T_c estimated via the McMillan

Composition	λ	ω_{log} (meV)	T_c^{**} (K)
Nd _{0.75} Sr _{0.25} NiO ₂ H _{0.25}	0.16	43.4	0
Nd _{0.80} Sr _{0.20} NiO ₂ H _{0.25} *	0.17	44.1	0
LaNiO ₂ H _{0.11}	0.21	33.0	0
LaNiO ₂ H _{0.22}	0.21	36.5	0
LaNiO ₂ H _{0.25}	0.21	42.8	0
LaNiO ₂ H _{0.55}	0.17	39.0	0

TABLE I. Summary of the calculated superconducting properties of various nickelate compounds with topotactic hydrogen. *: calculated by shifting the Fermi energy. **: calculated T_c 's below 1 mK are considered as zero.

formula is essentially zero [41, 42] and the T_c observed in Ref. [23] cannot be explained. To further rule out the unlikely event that the small difference in doping between the experimental compound (Nd_{0.8}Sr_{0.2}NiO₂H_{0.25}) and our calculations (Nd_{0.75}Sr_{0.25}NiO₂H_{0.25}) induces a significant change in T_c , we performed the same calculations for an effective 20% Sr doping [40] using a rigid-band approximation. The results are summarized in Tab. I; both λ and ω_{log} remain essentially identical and the resulting T_c is also zero.

Engineering optimal conditions for ep superconductivity in nickelates. In the previous section we discussed the absence of ep mediated superconductivity in Nd_{0.75}Sr_{0.25}NiO₂H_{0.25}. However, as previously noted, a stronger hydrogen character is present at about 0.5 eV above the Fermi level (Fig. 2), which might move towards the Fermi energy given a slight modification in the crystal structure and/or a higher electron filling. Since in superconducting hydrides the hydrogen character of states at the Fermi energy typically correlates with higher T_c 's [50, 51], this level of filling would appear more promising for the scenario of conventional superconductivity.

To explore this possibility and the effect of different rare earth cations, we studied different hydrogen configurations of the closely-related LaNiO₂H _{x} compound. Indeed, a hydrogen concentration of 25%, consistent with that reported in [23], yields an electronic structure that favors the previously outlined scenario. That is the bands with the largest hydrogen character that are 0.5 eV above the Fermi level for NdNiO₂H_{0.25} are crossing the Fermi energy for LaNiO₂H_{0.25} (see Supplemental Material [38] Fig. S5). We thus computed the vibrational and superconducting properties for four different topotactic hydrogen concentrations $x = 11\%$, 22% , and 55% (in a $3 \times 3 \times 1$ supercell), and 25% (in a $2 \times 2 \times 1$ supercell) for LaNiO₂H _{x} . A summary of these results is shown in Tab. I. Despite the more favorable conditions for ep mediated superconductivity, we find a total ep coefficient λ no higher than 0.21 in all the configurations investigated. Thereby we confirm that, albeit the contribution of hydrogen can be slightly more significant, the ep coupling remains low and cannot explain the observed T_c 's.

Our direct calculations of the ep coupling thus show that the Ni-H or Nd/La-H bonds do not contribute sufficiently to the ep coupling to explain the T_c 's measured by [23]. In NdNiO₂H_{0.25}, the ep mechanism is not particularly supported by the electronic structure, since no bands that cross the Fermi energy exhibit significant hydrogen character – an important ingredient for superconductivity in hydrides [50, 52]. However, even when the hydrogen bands are located at the Fermi energy they do not cause a significant T_c . This is most likely due to the ionic character of the La-H and Ni-H bonds [53], which cause the ep matrix elements to be small.

Enhanced T_c from Fermi surface nesting. Having established that the electron-phonon matrix elements are in general small, the only other scenario supporting conventional superconductivity could come from an enhancement due to Fermi surface nesting [39, 54]. On a qualitative level, the square-like sheet of the Fermi surface could indeed support this for phonons with wavevectors $\vec{q}_{nest} \sim (0.0, 0.4, 0.0)$ and $(0.4, 0.0, 0.0)$ [55].

To examine this possibility, we computed the Fermi surface nesting function, defined as in Refs. [44, 56], along a high-symmetry path (see Supplemental Material [38] Fig. S4), which presents two local maxima at X and M . Since these points were already present in the mesh used for the ep calculations, we also rule out nesting as a possible source of elusive ep interaction.

Conclusion. We investigated the possibility of topotactic hydrogen inducing superconductivity in nickelates through the conventional electron-phonon mechanism. Experimentally Sr-doped nickelates with a T_c of about 15 K appear to be extremely sensitive to the hydrogen concentration and some experiments suggest an s -wave gap that is to be expected in this scenario. Notwithstanding, we find that hydrogen does not strongly affect the states at the Fermi surface and that the ep coupling is too weak. The ep mediated T_c of Nd_{0.75}Sr_{0.25}NiO₂H_{0.25} is thus essentially zero.

To rule out that we missed the optimal conditions for ep mediated superconductivity, we further engineered the band structure by changing the rare-earth atom and hydrogen concentration. This did not yield any finite T_c either. Given the very weak ep coupling with $T_c < 1$ mK even under optimal conditions, we do not expect that many-body effects [18, 57–60] beyond our DF(P)T calculation such as quasi-particle renormalization, Hund's exchange on Ni, and modifications of crystal field splittings can enhance the T_c significantly. Consequently, we are inclined to conclude that hydrogen-derived phonons do not mediate superconductivity in infinite-layer nickelate superconductors. *Alternative explanations.* So why does a narrow range of hydrogen concentration appear to be essential for superconductivity in nickelates? One possibility is that (i) the inclusion of hydrogen changes the electronic structure and environment in a manner that is favorable for a mechanism different from conventional

ep coupling. However, currently, none of the proposed mechanisms for superconductivity in infinite-layer nickelates relies on the presence of hydrogen. On the contrary, it has been argued [18, 61] that the spin-1 state and three-dimensionality that is induced by topotactic hydrogen is unfavorable for superconductivity. Furthermore, it is at least somewhat unexpected that the window of hydrogen, where superconductivity is found, appears fairly small. With its agility, hydrogen will also tend to spread through the crystal and thus induce some disorder which is generally unfavorable for superconductivity.

Another possibility (ii) is that not only the hydrogen concentration is changed during the reduction process. Specifically, Ding *et al.* [23] use longer CaH₂ exposure times as a means to control the amount of intercalated H; and it is not unreasonable to surmise other aspects of the sample might alter as well. The most important is that these longer reduction times also affect the oxygen content which has to be reduced in the first place and which was not analyzed in Ref. [23]. The purported narrow range of hydrogen concentration might thus simply be the sweet spot of reduction time in Nd_{0.8}Sr_{0.2}NiO_{2+ δ} H _{x} with δ already sufficient low but x not yet too high for superconductivity — and $\delta = x = 0$ being the unreachable optimum.

Acknowledgments S.D.C. thanks Lilia Boeri for useful discussion, and Christoph Heil and Roman Lucrezi for sharing their code for calculating the anharmonic dynamical matrices. We acknowledge funding through the Austrian Science Funds (FWF) projects id I 5398, P 36213, SFB Q-M&S (FWF project ID F86), and Research Unit QUAST by the Deutsche Forschungsgemeinschaft (DFG; project ID FOR5249) and FWF (project ID I 5868). L.S. is thankful for the starting funds from Northwest University. Calculations have been done in part on the Vienna Scientific Cluster (VSC).

Data availability Raw data and our modifications to Quantum ESPRESSO are available at [XXX](#).

† simone.cataldo@tuwien.ac.at

- [1] D. Li, K. Lee, B. Y. Wang, M. Osada, S. Crossley, H. R. Lee, Y. Cui, Y. Hikita, and H. Y. Hwang, *Nature* **572**, 624 (2019).
- [2] M. Osada, B. Y. Wang, K. Lee, D. Li, and H. Y. Hwang, *Phys. Rev. Materials* **4**, 121801 (2020).
- [3] S. Zeng, C. Li, L. E. Chow, Y. Cao, Z. Zhang, C. S. Tang, X. Yin, Z. S. Lim, J. Hu, P. Yang, *et al.*, *Science advances* **8**, eabl9927 (2022).
- [4] M. Osada, B. Y. Wang, B. H. Goodge, S. P. Harvey, K. Lee, D. Li, L. F. Kourkoutis, and H. Y. Hwang, *Advanced Materials* **n/a**, 2104083 (2021).
- [5] G. A. Pan, D. F. Segedin, H. LaBollita, Q. Song, E. M. Nica, B. H. Goodge, A. T. Pierce, S. Doyle, S. Novakov, D. C. Carrizales, *et al.*, *Nature Materials* (2021), [10.1038/s41563-021-01142-9](#).

- [6] Let us also mention preceding theoretical calculations suggesting the possibility of superconductivity in nickelates superconductors [62] and heterostructures thereof [63–65].
- [7] Q. Gu, Y. Li, S. Wan, H. Li, W. Guo, H. Yang, Q. Li, X. Zhu, X. Pan, Y. Nie, and H.-H. Wen, *Nature Comm.* **11**, 6027 (2020).
- [8] L. E. Chow, S. K. Sudheesh, P. Nandi, S. Zeng, Z. Zhang, X. Du, Z. S. Lim, E. E. Chia, and A. Ariando, *arXiv preprint arXiv:2201.10038* (2022).
- [9] S. P. Harvey, B. Y. Wang, J. Fowlie, M. Osada, K. Lee, Y. Lee, D. Li, and H. Y. Hwang, *arXiv preprint arXiv:2201.12971* (2022).
- [10] X. Wu, D. Di Sante, T. Schwemmer, W. Hanke, H. Y. Hwang, S. Raghu, and R. Thomale, *Phys. Rev. B* **101**, 060504 (2020).
- [11] M. Kitatani, L. Si, O. Janson, R. Arita, Z. Zhong, and K. Held, *npj Quantum Materials* **5**, 59 (2020).
- [12] M. Kitatani, L. Si, P. Worm, J. M. Tomczak, R. Arita, and K. Held, *arXiv preprint arXiv:2207.14038* (2022).
- [13] J. Karp, A. Hampel, and A. J. Millis, *Phys. Rev. B* **105**, 205131 (2022).
- [14] A. Kreisel, B. M. Andersen, A. T. Rømer, I. M. Eremin, and F. Lechermann, *Phys. Rev. Lett.* **129**, 077002 (2022).
- [15] G.-M. Zhang, Y.-F. Yang, and F.-C. Zhang, *Phys. Rev. B* **101**, 020501 (2020).
- [16] P. Adhikary, S. Bandyopadhyay, T. Das, I. Dasgupta, and T. Saha-Dasgupta, *Phys. Rev. B* **102**, 100501 (2020).
- [17] M. Rossi, M. Osada, J. Choi, S. Agrestini, D. Jost, Y. Lee, H. Lu, B. Y. Wang, K. Lee, A. Nag, *et al.*, *Nature Physics* **18**, 869 (2022).
- [18] L. Si, W. Xiao, J. Kaufmann, J. M. Tomczak, Y. Lu, Z. Zhong, and K. Held, *Phys. Rev. Lett.* **124**, 166402 (2020).
- [19] Cf. [66, 67] for additional calculations showing topotactic hydrogen.
- [20] K. Lee, B. H. Goodge, D. Li, M. Osada, B. Y. Wang, Y. Cui, L. F. Kourkoutis, and H. Y. Hwang, *APL Materials* **8**, 041107 (2020).
- [21] Y. Cui, C. Li, Q. Li, X. Zhu, Z. Hu, Y. feng Yang, J. Zhang, R. Yu, H.-H. Wen, and W. Yu, *Chin. Phys. Lett.* **38**, 067401 (2021).
- [22] P. Puphal, V. Pomjakushin, R. A. Ortiz, S. Hammoud, M. Isobe, B. Keimer, and M. Hepting, *Frontiers in Physics* **10** (2022), 10.3389/fphy.2022.842578.
- [23] X. Ding, C. C. Tam, X. Sui, Y. Zhao, M. Xu, J. Choi, H. Leng, J. Zhang, M. Wu, H. Xiao, X. Zu, M. Garcia-Fernandez, S. Agrestini, X. Wu, Q. Wang, P. Gao, S. Li, B. Huang, K.-J. Zhou, and L. Qiao, *Nature* **615**, 50 (2023).
- [24] A. P. Drozdov, M. I. Erements, I. A. Troyan, V. Ksenofontov, and S. I. Shylin, *Nature* **525**, 73 (2015).
- [25] M. Einaga, M. Sakata, T. Ishikawa, K. Shimizu, M. Erements, A. P. Drozdov, I. A. Troyan, N. Hirao, and Y. Ohishi, *Nature Physics* **12**, 835 (2016).
- [26] M. Somayazulu, M. Ahart, A. K. Mishra, Z. M. Geballe, M. Baldini, Y. Meng, V. V. Struzhkin, and R. J. Hemley, *Phys. Rev. Lett.* **122**, 027001 (2019).
- [27] L. Boeri and G. B. Bachelet, *J. Phys.: Condens. Matter* **31**, 234002 (2019).
- [28] C. J. Pickard, I. Errea, and M. Erements, *Annual Review of Condensed Matter Physics* **11**, 57 (2020).
- [29] Y. Nomura, M. Hirayama, T. Tadano, Y. Yoshimoto, K. Nakamura, and R. Arita, *Phys. Rev. B* **100**, 205138 (2019).
- [30] L. Si, W. Xiao, J. Kaufmann, J. M. Tomczak, Y. Lu, Z. Zhong, and K. Held, *Phys. Rev. Lett.* **124**, 166402 (2020).
- [31] L. Si, P. Worm, and K. Held, *arXiv:2208.11085* .
- [32] K. Lee, B. Y. Wang, M. Osada, B. H. Goodge, T. C. Wang, Y. Lee, S. Harvey, W. J. Kim, Y. Yu, C. Murthy, *et al.*, *arXiv preprint arXiv:2203.02580* (2022).
- [33] P. Hohenberg and W. Kohn, *Phys. Rev.* **136**, B864 (1964).
- [34] S. Baroni, S. de Gironcoli, A. Dal Corso, and P. Gianozzi, *Rev. Mod. Phys.* **73**, 515 (2001).
- [35] D. R. Hamann, *Phys. Rev. B* **88**, 085117 (2017).
- [36] M. J. van Setten, M. Giantomassi, E. Bousquet, M. J. Verstraete, D. R. Hamann, X. Gonze, and G.-M. Rignanese, *Computer Physics Communications* **226**, 39 (2018).
- [37] K. Momma and F. Izumi, *J. Appl. Cryst.* **41**, 653 (2008).
- [38] [URL_will_be_inserted_by_publisher](#), the supplementary material is available at..
- [39] C. Heil, S. Poncé, H. Lambert, M. Schlipf, E. R. Margine, and F. Giustino, *Phys. Rev. Lett.* **119**, 087003 (2017).
- [40] This calculation was performed with an in-house modified version of **Quantum ESPRESSO**. The modified code is available in accordance with the GNU license at the **XXX** repository.
- [41] W. L. McMillan, *Phys. Rev.* **167**, 331 (1968).
- [42] P. B. Allen and R. C. Dynes, *Phys. Rev. B* **12**, 905 (1975).
- [43] F. Giustino, M. L. Cohen, and S. G. Louie, *Phys. Rev. B* **76**, 165108 (2007).
- [44] S. P. and E. R. Margine, C. Verdi, and F. Giustino, *Comp. Phys. Communications* **209**, 116 (2016).
- [45] P. Jiang, L. Si, Z. Liao, and Z. Zhong, *Phys. Rev. B* **100**, 201106 (2019).
- [46] P. Giannozzi, S. Baroni, N. Bonini, M. Calandra, R. Car, C. Cavazzoni, D. Ceresoli, G. L. Chiarotti, M. Cococcioni, and I. Dabo, *J. Phys.: Condens. Matter* **21**, 395502 (2009).
- [47] P. Giannozzi, O. Andreussi, T. Brumme, O. Bunau, M. B. Nardelli, M. Calandra, R. Car, C. Cavazzoni, D. Ceresoli, M. Cococcioni, *et al.*, *J. Phys.: Condens. Matter* **29**, 465901 (2017).
- [48] S. Baroni, S. de Gironcoli, A. D. Corso, and P. Giannozzi, *Rev. Mod. Phys.* **73**, 515 (2001).
- [49] The imaginary frequencies are plotted as negative in Fig. 3.
- [50] F. Belli, T. Novoa, J. Contreras-Garcia, and I. Errea, *Nature Communications* **12**, 5381 (2021).
- [51] L. Boeri, R. Hennig, P. Hirschfeld, G. Profeta, A. Sanna, E. Zurek, W. E. Pickett, M. Amsler, R. Dias, M. I. Erements, *et al.*, *J. Phys. Condens. Matter* **34**, 183002 (2021).
- [52] C. Heil, G. B. Bachelet, and L. Boeri, *Phys. Rev. B* **97**, 214510 (2018).
- [53] C. Heil and L. Boeri, *Phys. Rev. B* **92**, 060508(R) (2015).
- [54] W. Kohn, *Phys. Rev. Lett.* **2**, 393 (1959).
- [55] This wave vector is different from the one observed in resonant inelastic x-ray scattering (RIXS) [68, 69].
- [56] C. Heil, H. Sormann, L. Boeri, M. Aichhorn, and W. von der Linden, *Phys. Rev. B* **90**, 115143 (2014).
- [57] F. Petocchi, V. Christiansson, F. Nilsson, F. Aryasetiawan, and P. Werner, *Phys. Rev. X* **10**, 041047 (2020).
- [58] Y. Wang, C.-J. Kang, H. Miao, and G. Kotliar, *Phys. Rev. B* **102**, 161118 (2020).

- [59] H. LaBollita, M.-C. Jung, and A. S. Botana, *Phys. Rev. B* **106**, 115132 (2022).
- [60] G. Pascut, L. Cosovanu, K. Haule, and K. F. Quader, *Commun. Phys.* **6**, 45 (2023).
- [61] M. Jiang, M. Berciu, and G. A. Sawatzky, *Phys. Rev. Lett.* **124**, 207004 (2020).
- [62] V. I. Anisimov, D. Bukhvalov, and T. M. Rice, *Phys. Rev. B* **59**, 7901 (1999).
- [63] J. Chaloupka and G. Khaliullin, *Physical Review Letters* **100**, 016404 (2008).
- [64] P. Hansmann, X. Yang, A. Toschi, G. Khaliullin, O. K. Andersen, and K. Held, *Phys. Rev. Lett.* **103**, 016401 (2009).
- [65] P. Hansmann, A. Toschi, X. Yang, O. Andersen, and K. Held, *Phys. Rev. B* **82**, 235123 (2010).
- [66] O. I. Malyi, J. Varignon, and A. Zunger, *Phys. Rev. B* **105**, 014106 (2022).
- [67] F. Bernardini, A. Bosin, and A. Cano, *Phys. Rev. Materials* **6**, 044807 (2022).
- [68] G. Krieger, L. Martinelli, S. Zeng, L. E. Chow, K. Kummer, R. Arpaia, M. Moretti Sala, N. B. Brookes, A. Ariando, N. Viart, M. Salluzzo, G. Ghiringhelli, and D. Preziosi, *Phys. Rev. Lett.* **129**, 027002 (2022).
- [69] C. C. Tam, J. Choi, X. Ding, S. Agrestini, A. Nag, M. Wu, B. Huang, H. Luo, P. Gao, M. García-Fernández, *et al.*, *Nature Materials* **21**, 1116 (2022).